IOP Publishing Smart Materials and Structures
Smart Mater. Struct. **23** (2014) 125014 (11pp) doi:10.1088/0964-1726/23/12/125014

Piezoelectric vibration damping using resonant shunt circuits: an exact solution

P Soltani[1,3], G Kerschen[1], G Tondreau[2] and A Deraemaeker[2]

[1] Space Structures and Systems Laboratory, Department of Aerospace and Mechanical Engineering, University of Liège, Liège, Belgium
[2] Building Architecture and Town Planning (BATir), Universitè Libre de Bruxelles, Brussels, Belgium

E-mail: payam.soltani@ulg.ac.be, g.kerschen@ulg.ac.be, gilles.tondreau@ulb.ac.be and aderaema@ulb.ac.be

Received 1 July 2014, revised 24 September 2014
Accepted for publication 24 September 2014
Published 27 October 2014

Abstract

The objective of this paper is to propose an exact closed-form solution to the H_∞ optimization of piezoelectric materials shunted with inductive-resistive passive electrical circuits. Realizing that Den Hartog's method which imposes fixed points of equal height in the receptance transfer function is approximate, the parameters of the piezoelectric tuned vibration absorber are calculated through the direct minimization of the maxima of the receptance. The method is applied to a one-degree-of-freedom primary oscillator considering various values of the electromechanical coupling coefficients.

Keywords: piezoelectric tuned vibration absorber, shunted piezoelectric transducer, optimum tuning rule, equal-peak method, exact closed-form solution

1. Introduction

The mechanical tuned vibration absorber (MTVA) is probably the most popular passive anti-vibration device [1]. Successful applications of the MTVA can be found in civil engineering structures (e.g., the Burj Al Arab Hotel in Dubai, the Taipei World Financial Center in Taiwan and the Millenium Bridge in London) and in other engineering applications (e.g., cars and high-voltage lines). Different studies contributed to the development of analytic tuning procedures for the MTVA starting from the work of Den Hartog [2] and Brock [3] to the more recent contributions of Asami and Nishihara [4, 5].

An interesting alternative to the MTVA is the piezoelectric tuned vibration absorber (PTVA) implemented with a piezoelectric transducer (PZT) bonded to the structure and shunted with an electrical impedance. As the structure deforms, the PZT converts a portion of the mechanical energy into electrical energy which is in turn dissipated by the electrical circuit. Resonant circuit shunting is most often considered where the inherent capacitance of the PZT is shunted with a resistor and an inductor [6]. Linear [7, 8] and nonlinear [9–11] shunting strategies have been proposed in the literature. Even if they have their own limitations, PTVAs possess several advantages with respect to MTVAs, such as the absence of moving parts and the possibility to be fine-tuned online to compensate for any modeling errors. For instance, PTVAs have been proposed for bladed disks assemblies, see, e.g., [12–15].

Resonant circuit shunting enhances piezoelectric vibration damping through appropriate values of the frequency tuning and damping parameters. In [7], two different methods were proposed relying on the receptance transfer function and on pole placement, respectively. The former rule extends Den Hartog's fixed-point method [2] to PTVAs and is widely used in the literature [16]. Minimization of the frequency response amplitude is achieved by selecting the frequency tuning parameter that gives two fixed points in the receptance of the primary structure of equal heights. The later rule maximizes the attainable modal damping by finding the value of the frequency tuning parameter for which the distinct poles coalesce in double complex conjugate pairs. Hogsberg and Krenk recently proposed a tuning rule that is a balanced compromise between these two design criteria [17]. Through the development of an equivalent mechanical model of a piezoelectric element, Yamada *et al* [18] introduced a new approximate

[3] Space Structures and Systems Laboratory, Department of Aerospace and Mechanical Engineering, University of Lige, 1 Chemin des Chevreuils (B52/3), B-4000 Liège, Belgium.

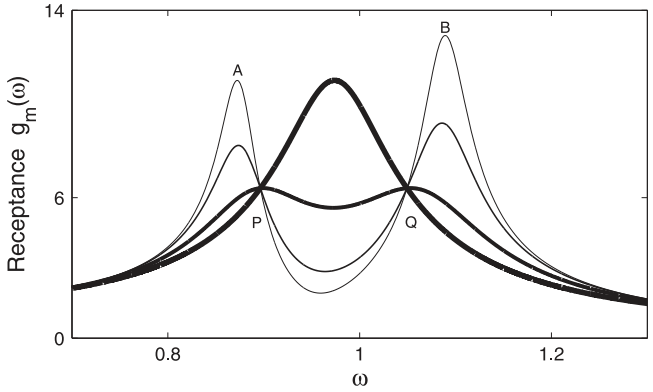

Figure 1. Illustration of Den Hartog's fixed-point method for $\beta = 0.05$, $\delta_m = 0.952$ and for various absorber damping values ($\xi_2 = 0.0447$, $\xi_2 = 0.067$, $\xi_{2,opt} = 0.134$ and $\xi_2 = 0.268$; line thicknesses are proportion to ξ_2).

analytic expression for the damping parameter that improves the PTVA performance compared to the formulae proposed in [7].

Because all the aforementioned tuning rules are approximate, the contribution of the present paper is to derive an exact closed-form solution for the design of piezoelectric vibration absorbers based on resonance circuit shunting. The paper is organized as follows. Section 1 briefly reviews Den Hartog's fixed-point method for MTVAs together with the exact solution proposed by Asami and Nishihara [4]. In section 3, the formulation for shunted PZTs is introduced, and the tuning rules proposed by Hagood and von Flotow [7] and Yamada and co-workers [18] are discussed. An exact tuning rule for PTVAs is derived in section 4 and compared to the other tuning rules using a one-degree-of-freedom mechanical oscillator. Finally, the conclusions of the present study are drawn in section 5.

2. The mechanical tuned vibration absorber

The steady-state response of an undamped mass–spring system subjected to a harmonic excitation at a constant frequency can be suppressed using an undamped tuned vibration absorber (TVA), as proposed by Frahm in 1909 [19]. However, the TVA performance deteriorates significantly when the excitation frequency varies. To improve the performance robustness, damping was introduced in the absorber by Ormondroyd and Den Hartog [20]. The equations of motion of the coupled system are

$$\begin{aligned} m_1\ddot{x} + k_1 x + c_2\left(\dot{x}-\dot{y}\right) + k_2(x-y) &= f\,\sin\omega t,\\ m_2\ddot{y} + c_2\left(\dot{y}-\dot{x}\right) + k_2(y-x) &= 0, \end{aligned} \tag{1}$$

where $x(t)$ and $y(t)$ are the displacements of the harmonically-forced undamped primary system and of the MTVA, respectively. k_1 and k_2 are the stiffness of the primary structure and of the MTVA, in that order. c_2 represents the damping of the MTVA.

Table 1. Amplitude of the fixed-points and maxima of the receptance transfer function for Den Hartog's tuning rule ($m_1 = 1$ kg and $k_1 = 1$ N m^{-1}).

Mass ratio	Fixed point P	Fixed point Q	Maximum A	Maximum B
0.05	6.4031	6.4031	6.4075	6.4084
0.1	4.5826	4.5826	4.5884	4.5902
0.5	2.2361	2.2361	2.2453	2.2530
1.0	1.7321	1.7321	1.7417	1.7544

Den Hartog demonstrated that the receptance $g_m(\omega)$ of the primary mass passes through two fixed points independent of absorber damping, as illustrated in figure 1. He proposed a tuning rule that provides two fixed points of equal height in the receptance curve [2]. Brock then computed the optimum damping by taking the mean of the damping values that realize a maximum of the receptance at the two fixed points [3]. The corresponding analytic formulae for the frequency tuning δ_m and damping ξ_2 ratios are:

$$\begin{aligned} \delta_m &= \frac{\omega_2}{\omega_1} = \frac{1}{1+\beta},\\ \xi_2 &= \frac{c_2}{2\sqrt{k_2 m_2}} = \sqrt{\frac{3\beta}{8(1+\beta)}}, \end{aligned} \tag{2}$$

where ω_1 and ω_2 are the natural frequencies of the primary system and of the absorber, respectively, $\beta = m_2/m_1$ is the mass ratio and ξ_2 is the damping ratio. Table 1 shows that the two fixed points have the same amplitudes, unlike the two maxima of the receptance curve. Even though they have most likely sufficient accuracy considering the uncertainty inherent to practical applications, formulas (2) are therefore only approximate.

Interestingly, it is only recently that an exact closed-form solution to this classical problem could be found [4]. Instead of imposing two fixed points of equal amplitude, the direct minimization of the H_∞ norm of the frequency response of the controlled structure is achieved:

$$\min \;\| g_m(\omega) \|_\infty \rightarrow \left| g_m(\omega_A) \right| = \| \left| g_m(\omega_B) \right|, \tag{3}$$

where ω_A and ω_B represent the resonance frequencies. Eventually, exact analytic formulas can be obtained for the frequency tuning and damping ratios:

$$\begin{aligned} \delta_m &= \frac{2}{1+\beta}\sqrt{\frac{2\left[16+23\beta+9\beta^2+2(2+\beta)\sqrt{4+3\beta}\right]}{3\left(64+80\beta+27\beta^2\right)}}\\ \xi_2 &= \frac{1}{4}\sqrt{\frac{8+9\beta-4\sqrt{4+3\beta}}{1+\beta}}. \end{aligned} \tag{4}$$

Table 2 confirms that this tuning rule yields resonance peaks of equal amplitude. It also shows that, for this optimum design, the fixed points of the receptance curve do not have the same amplitude.

We note that all the developments in this section assume an undamped primary system. To date, there is no exact

Table 2. Amplitude of the fixed-points and maxima of the receptance transfer function for Asami and Nishihara's tuning rule ($m_1 = 1$ kg and $k_1 = 1$ N m^{-1}).

Mass ratio	Fixed point P	Fixed point Q	Maximum A	Maximum B
0.05	6.4027	6.4035	6.4079	6.4079
0.1	4.5819	4.5833	4.5892	4.5892
0.5	2.2334	2.2387	2.2480	2.2480
1.0	1.7281	1.7360	1.7456	1.7456

solution for damped primary systems, but accurate approximate analytic formulas have been derived [5].

3. The piezoelectric vibration absorber: existing tuning rules

3.1. Governing equations of structures with shunted piezoelectric materials

Because we aim at mitigating one specific structural resonance, a one-degree-of-freedom modal model of the host structure, assumed to be undamped, is considered to which a shunted PZT is attached. The PZT shunt is a series *RL* circuit. This system is schematized in figure 2.

Assuming linear characteristics under constant temperature, the general form of the piezoelectric constitutive equations are standardized by IEEE [21]:

$$\begin{aligned}\mathbf{S} &= [d]\mathbf{E} + \left[s^E\right]\mathbf{T},\\ \mathbf{D} &= \left[\epsilon^T\right]\mathbf{E} + [d]^*\mathbf{T}.\end{aligned} \tag{5}$$

where $\mathbf{T}$ and $\mathbf{S}$ are the material stress and strain vectors, respectively; $\left[s^E\right]$ is the compliance matrix of the piezoceramic under constant electric field; $\left[\epsilon^T\right]$ represents the permittivity under constant stress; $[d]$ is the matrix of piezoelectric constants, and $*$ denotes matrix transpose. The components of the aforementioned vectors and matrices for a general 3D problem are described in [7]. The current problem considers the PZT rod as a one-dimensional element in which both the expansion and polarization direction coincidence with the central axis of the rod (conventionally called the '3'-direction). Hence, the PZT rod operates in its thickness transduction mode or d_{33}-mode. The constitutive equations of the PZT rod then become:

$$\begin{Bmatrix} D_3 \\ S_{33} \end{Bmatrix} = \begin{bmatrix} \epsilon_3^T & d_{33} \\ d_{33} & s_{33}^E \end{bmatrix} \begin{Bmatrix} E_3 \\ T_3 \end{Bmatrix}. \tag{6}$$

By integrating equations (6) over the volume of the PZT rod, the charge q and the displacement x are written as functions of the force f_{PZT} and the voltage between the electrodes v_{PZT}:

$$\begin{Bmatrix} q \\ x \end{Bmatrix} = \begin{bmatrix} c_{\mathrm{PZT}} & d_{33} \\ d_{33} & \dfrac{1}{k_{\mathrm{PZT}}} \end{bmatrix} \begin{Bmatrix} v_{\mathrm{PZT}} \\ f_{\mathrm{PZT}} \end{Bmatrix}. \tag{7}$$

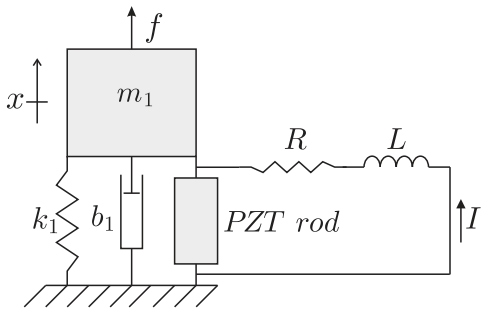

Figure 2. Piezoelectric vibration absorber with a series *RL* shunt.

The coefficient c_{PZT} is the capacitance between the electrodes of the PZT rod with no external force, and k_{PZT} is the stiffness of the short-circuited PZT rod. They are defined as:

$$c_{\mathrm{PZT}} = \epsilon_3^T \frac{s_0}{l_0}, \quad k_{\mathrm{PZT}} = \frac{1}{s_{33}^E}\frac{s_0}{l_0}, \tag{8}$$

where s_0 and l_0 are the cross section area and length of the PZT rod, respectively. Equation (7) can be reformulated as:

$$\begin{Bmatrix} v_{\mathrm{PZT}} \\ f_{\mathrm{PZT}} \end{Bmatrix} = \begin{bmatrix} \dfrac{1}{\bar{c}_{\mathrm{PZT}}} & -\theta \\ -\theta & \bar{k}_{\mathrm{PZT}} \end{bmatrix} \begin{Bmatrix} q \\ x \end{Bmatrix}. \tag{9}$$

where

$$\begin{aligned}\bar{c}_{\mathrm{PZT}} &= c_{\mathrm{PZT}}\left(1 - k_0^2\right),\\ \bar{k}_{\mathrm{PZT}} &= \frac{k_{\mathrm{PZT}}}{1 - k_0^2},\\ \theta &= \frac{k_0}{1 - k_0^2}\sqrt{\frac{k_{\mathrm{PZT}}}{c_{\mathrm{PZT}}}},\end{aligned} \tag{10}$$

are the capacitance of the PZT rod under constant strain, the stiffness of the PZT rod with open electrodes, and the electromechanical coupling factor θ, respectively. These parameters are defined as functions of the electromechanical coupling coefficient in d_{33}-mode:

$$k_0 = d_{33}\sqrt{\frac{k_{\mathrm{PZT}}}{c_{\mathrm{PZT}}}} = d_{33}\frac{1}{\sqrt{s_{33}^E \epsilon_3^T}}. \tag{11}$$

Finally, placing a resistive–inductive (*RL*) shunt across the electrodes of the piezoelectric and applying Newton's and Kirchhoff's law yield the governing equations of the

system:

$$m_1\ddot{x} + \left(k_1 + \bar{k}_{\mathrm{PZT}}\right)x - \theta q = f\,\sin\omega t,$$
$$L\ddot{q} + R\dot{q} + \bar{c}_{\mathrm{PZT}}^{-1}\,q - \theta x = 0, \tag{12}$$

where the primary host structurer is considered undamped (i.e. $b_1 = 0$). By defining the parameters similarly to [9]:

$$\omega_1 = \sqrt{\frac{k_1 + \bar{k}_{\mathrm{PZT}}}{m_1}}, \quad \omega_e = \frac{1}{\sqrt{L\,\bar{c}_{\mathrm{PZT}}}},$$
$$\gamma = \frac{\omega}{\omega_1}, \quad \delta = \frac{\omega_e}{\omega_1},$$
$$\tilde{x} = \sqrt{m_1}\,x, \quad \tilde{q} = \sqrt{L}\,q,$$
$$r = R\,\bar{c}_{\mathrm{PZT}}\,\omega_1, \quad \tau = \omega_1 t,$$
$$f_0 = \frac{f}{\omega_1\sqrt{\bar{k}_{\mathrm{PZT}} + k_1}}, \quad \alpha = \theta\sqrt{\frac{\bar{c}_{\mathrm{PZT}}}{\bar{k}_{\mathrm{PZT}} + k_1}}, \tag{13}$$

equations (12) can be conveniently recast into

$$\tilde{x}'' + \tilde{x} - \delta\alpha\tilde{q} = f_0\,\sin\gamma\tau$$
$$\tilde{q}'' + r\delta^2\tilde{q}' - \delta\alpha\tilde{x} + \delta^2\tilde{q} = 0, \tag{14}$$

where prime denotes differentiation with respect to the dimensionless time τ. We note that the parameter

$$\alpha = \theta\sqrt{\frac{\bar{c}_{\mathrm{PZT}}}{\bar{k}_{\mathrm{PZT}} + k_1}} = \sqrt{\frac{k_0^2}{1-k_0^2}}\sqrt{\frac{k_{\mathrm{PZT}}}{\bar{k}_{\mathrm{PZT}} + k_1}}$$
$$= k_0\sqrt{\frac{\bar{k}_{\mathrm{PZT}}}{\bar{k}_{\mathrm{PZT}} + k_1}} = \frac{k_0}{\sqrt{1+\kappa}}, \tag{15}$$

depends only on the stiffness ratio $\kappa = k_1/\bar{k}_{\mathrm{PZT}}$ and the electromechanical coupling coefficient k_0. Since PZT rods typically have $k_0 \cong 0.7$ in d_{33}-mode, α takes values between 0 and 0.7. It is related to the generalized electromechanical coupling coefficient K_{ij} defined in [7] according to the relation

$$K_{ij} = \sqrt{\frac{k_0^2}{1-k_0^2}}\sqrt{\frac{k_{\mathrm{PZT}}}{k_{\mathrm{PZT}} + k_1}} \rightarrow K_{ij} = \alpha\sqrt{\frac{1+\kappa}{1-k_0^2+\kappa}} \tag{16}$$

3.2. Tuning rules for resonant shunt circuits

Given a value of the parameter α, the tuning of a *RL* shunt requires to determine the frequency tuning δ and damping r parameters. As briefly discussed in the introductory section, different rules exist for finding appropriate values of these parameters. Two methods that apply Den Hartog's fixed-point method to PTVAs, namely those of Hagood and von Flotow [7] and Yamada *et al* [18], are described in this section.

3.2.1. Hagood's tuning rule. In 1991, Hagood and von Flotow introduced the first tuning method for resonant shunt circuits based on the receptance transfer function of the primary mass:

$$g_e(\gamma) = \left|\frac{\tilde{x}}{f_0}\right|$$
$$= \left|\frac{j\delta^2 r\gamma + \delta^2 - \gamma^2}{\gamma^4 - j\delta^2 r\gamma^3 - \left(\delta^2+1\right)\gamma^2 + j\delta^2 r\gamma + \left(1-\alpha^2\right)\delta^2}\right|, \tag{17}$$

with $j = \sqrt{-1}$. Since then, this method has often been used in the literature (e.g., Inman and co-workers applied the method for tuning the linear part of the proposed nonlinear piezoelectric shunt [9]).

The first step consists in selecting the frequency tuning parameter δ that yields two fixed points of equal amplitude in the receptance $g_{\mathrm{e}}(\gamma)$. At the fixed points, the open circuit ($r = \infty$) and the closed circuit ($r = 0$) receptance function should be coincident. Solving the equation:

$$g_{\mathrm{e}}(\gamma)\Big|_{r=0} = g_{\mathrm{e}}(\gamma)\Big|_{r=\infty}, \tag{18}$$

yields the dimensionless frequencies of the fixed points P and Q:

$$\gamma_{P,Q} = \frac{\sqrt{2}}{2}\,\frac{\sqrt{\delta^2 + 1 \pm \sqrt{\delta^4 + 2\,\delta^2\alpha^2 - 2\,\delta^2 + 1}}}{\delta}. \tag{19}$$

The optimum value $\delta_{\mathrm{opt}} = 1$ is subsequently obtained by imposing

$$g_{\mathrm{e}}(\gamma_{P,Q}) = g_{\mathrm{e}}(\gamma_{P,Q})\Big|_{r=\infty}. \tag{20}$$

Because the parameters (13) are somewhat different from those considered in [7], the value of δ_{opt} is also different. At the optimum, the frequency of the fixed points and the corresponding amplitudes of the transfer function are

$$\gamma_{P,Q} = \frac{\sqrt{2}}{2}\sqrt{2 \pm \sqrt{2}\,\alpha} \text{ and } g_{\mathrm{e}}(\gamma_P) = g_{\mathrm{e}}(\gamma_Q) = \frac{\sqrt{2}}{\alpha} \tag{21}$$

Determining the optimal circuit damping is more challenging. To this end, Hagood and von Flotow proposed to set

$$g_{\mathrm{e}}(\gamma_{P,Q}) = g_{\mathrm{e}}(\delta_{\mathrm{opt}}). \tag{22}$$

As we shall see, this expression is approximate. Combining equations (17), (21) and (22) yields

$$r_{\mathrm{opt}_H} = \sqrt{2}\,\alpha. \tag{23}$$

3.2.2. Yamada's tuning rule. Through the development of an equivalent mechanical model of a piezoelectric element, Yamada *et al* [18] improved the analytic approximations proposed in [7]. Specifically, they still consider the value $\delta_{\mathrm{opt}} = 1$ for the frequency tuning, but the damping ratio of the PTVA is derived such that the derivative of the receptance $g_{\mathrm{e}}(\gamma)$ should be zero at the

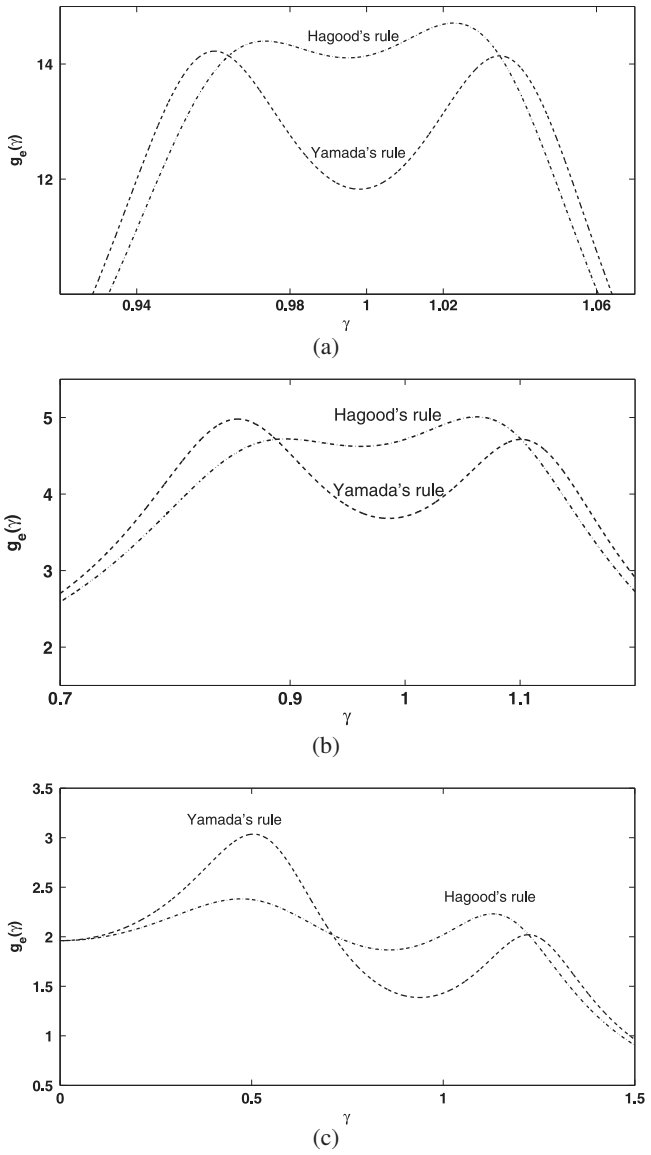

Figure 3. Performance of existing tuning rules for PTVAFs for different values of α. (a) $\alpha = 0.1$, $r_{\mathrm{opt}_Y} = 0.1184$, $r_{\mathrm{opt}_H} = 0.1414$, $\delta = 1$. (b) $\alpha = 0.3$, $r_{\mathrm{opt}_Y} = 0.3337$, $r_{\mathrm{opt}_H} = 0.4243$, $\delta = 1$. (c) $\alpha = 0.7$, $r_{\mathrm{opt}_Y} = 0.7012$, $r_{\mathrm{opt}_H} = 0.9899$, $\delta = 1$.

fixed points:

$$\left.\frac{\mathrm{d}g_e(\gamma)}{\mathrm{d}\gamma}\right|_{\gamma_P,\gamma_Q} = 0. \tag{24}$$

By substituting equation (21) into equation (24), two different optimum circuit damping values are calculated for points P and Q:

$$r_{P,Q} = \frac{\sqrt{3}}{\sqrt[4]{2}}\frac{\alpha}{\sqrt{\sqrt{2} \pm \alpha}}. \tag{25}$$

meaning that the two maxima of $g_e(\gamma)$ cannot simultaneously coincide with the fixed points. They proposed to define the optimum value through the root mean square:

$$r_{\mathrm{opt}_Y} = \sqrt{\frac{r_P^2 + r_Q^2}{2}} = \frac{\sqrt{3}\,\alpha}{\sqrt{2-\alpha^2}}. \tag{26}$$

The performance of the two tuning rules are illustrated in figure 3 for different dimensionless coupling parameters α. For $\alpha = 0.1$, the rule proposed by Yamada *et al* provides two peaks of almost identical amplitudes, whereas the rule of Hagood and von Flotow is less accurate. For larger values of α, none of these rules provides equal peaks in the receptance function.

4. The piezoelectric vibration absorber: exact tuning rule

4.1. Theory

As discussed in section 2 for MTVAs and as also shown in the previous section, a fixed-point-based absorber design cannot yield resonance peaks of equal amplitude. Following the method proposed by Nishihara and Asami [4] for MTVAs, an exact solution for the H_∞ optimization of piezoelectric materials shunted with resistive-inductive passive electrical circuits is derived in this section. It is obtained by focusing only on the resonant points A and B, therefore ignoring the existence of the fixed points. So, for a given value of α

$$\min_{\delta,r} \left\| g_e(\gamma) \right\|_\infty \rightarrow \text{find } \delta,\ r \text{ such that}$$
$$\left| g_e(\gamma_A) \right| = \left| g_e(\gamma_B) \right| \equiv h_0. \tag{27}$$

For simplicity, the square of the receptance function $g_e^2(\gamma) = n(\gamma)/d(\gamma)$ is considered where

$$n(\gamma) = 1 + \gamma^4 + \left(\delta^2 r^2 - 2\right)\gamma^2, \tag{28}$$

$$\begin{aligned} d(\gamma) = {} & \delta^4\gamma^8 + \left(\delta^6 r^2 - 2\,\delta^4 - 2\delta^2\right)\gamma^6 \\ & + \left(-2\,\delta^4 r^2 - 2\alpha^2\delta^2 + \delta^4 + 4\,\delta^2 + 1\right)\gamma^4 \\ & + \left(2\,\alpha^2\delta^2 + \delta^2 r^2 + 2\alpha^2 - 2\,\delta^2 - 2\right) \\ & \times \gamma^2 + \alpha^4 - 2\,\alpha^2 + 1. \end{aligned} \tag{29}$$

Because only terms of even power appear in these expressions, we can pose $\gamma_1 = \gamma^2$ such that $g_e^2(\gamma_1) = N(\gamma_1)/D(\gamma_1)$ with

$$\begin{aligned} N(\gamma_1) = {} & 1 + \gamma_1^2 + \left(\delta^2 r^2 - 2\right)\gamma_1, \\ D(\gamma_1) = {} & \delta^4\gamma_1^4 + \left(\delta^6 r^2 - 2\,\delta^4 - 2\,\delta^2\right)\gamma_1^3 \\ & + \left(-2\,\delta^4 r^2 - 2\,\alpha^2\delta^2 + \delta^4 + 4\,\delta^2 + 1\right)\gamma_1^2 \\ & + \left(2\,\alpha^2\delta^2 + \delta^2 r^2 + 2\,\alpha^2 - 2\,\delta^2 - 2\right) \\ & \times \gamma_1 + \alpha^4 - 2\,\alpha^2 + 1. \end{aligned} \tag{30}$$

Following the definition of $N(\gamma_1)$ and $D(\gamma_1)$, the fourth-order polynomial is obtained

$$F(\gamma_1) = D(\gamma_1) - \frac{N(\gamma_1)}{h_0^2}, \tag{31}$$

equation (27) shows that two obvious roots of this polynomial are γ_{1A} and γ_{1B}. Because the receptance transfer function possesses horizontal tangents at the resonant points A and B, it also follows that

$$F'(\gamma_{1A}) = F'(\gamma_{1B}) = 0, \tag{32}$$

where prime represents the derivative with respect to γ_1. According to equation (32), the multiplicity of the roots γ_{1A} and γ_{1B} is two:

$$\begin{aligned} F(\gamma_1) &= \gamma_1^4 + b_1\gamma_1^3 + b_2\gamma_1^2 + b_3\gamma_1 + b_4 \\ &= (\gamma_1 - \gamma_{1A})^2(\gamma_1 - \gamma_{1B})^2, \end{aligned} \tag{33}$$

with the coefficients b_i defined as

$$\begin{aligned} b_1 &= -2\left(\gamma_{1A} + \gamma_{1B}\right), \\ b_2 &= \left(\gamma_{1A} + \gamma_{1B}\right)^2 + 2\gamma_{1A}\gamma_{1B}, \\ b_3 &= -2\gamma_{1A}\gamma_{1B}\left(\gamma_{1A} + \gamma_{1B}\right), \\ b_4 &= \gamma_{1A}^2\gamma_{1B}^2. \end{aligned} \tag{34}$$

It follows that

$$\begin{aligned} f_1 &= b_1\sqrt{b_4} - b_3 = 0, \\ f_2 &= \frac{b_1^2}{4} + 2\sqrt{b_4} - b_2 = 0. \end{aligned} \tag{35}$$

By substituting the expression of $N(\gamma_1)$ and $D(\gamma_1)$ from equations (30) into (31), another expression of the coefficients bi can be obtained:

$$\begin{aligned} b_1 &= -2 - 2\,\delta_1 + \frac{r_1}{\delta_1}, \\ b_2 &= \delta_1^2 h_1^2 + (4 - 2\,\alpha_1)\delta_1 - 2\,r_1 + 1, \\ b_3 &= \delta_1\left[\left(-2\,h_1^2 + 2\,\alpha_1\right)\delta_1 + h_1^2 r_1 + 2\,\alpha_1 - 2\right], \\ b_4 &= \delta_1^2\left(h_1^2 + \alpha_1^2 - 2\,\alpha_1\right), \end{aligned} \tag{36}$$

where $h_1^2 = 1 - 1/h_0^2$, $\delta_1 = 1/\delta^2$, $r_1 = r^2$ and $\alpha_1 = \alpha^2$. Equations (35) therefore becomes

$$\begin{aligned} f_1 &= \left(-2\,\delta_1^2 + r_1 - 2\,\delta_1\right)\chi \\ &\quad -\delta_1\left[\left(-2\,h_1^2 + 2\,\alpha_1\right)\delta_1 + h_1^2 r_1 + 2\,\alpha_1\right] = 0, \end{aligned} \tag{37}$$

$$\begin{aligned} f_2 &= \left(1 - h_1^2\right)\delta_1^4 + 2(\chi + \alpha_2 - 1)\delta_1^3 \\ &\quad + r_1\,\delta_1^2 - r_1\,\delta_1 + \frac{1}{4}r_1^2 = 0, \end{aligned} \tag{38}$$

where $\chi \equiv \sqrt{h_1^2 + \alpha_1^2 - 2\,\alpha_1}$.

Equation (37) is solved for r_1 equal to the square of the optimum circuit damping:

$$r_1 = \frac{2\,\delta_1\left[-\delta_1\,h_1^2 + \delta_1\,\chi + \delta_1\,\alpha_1 + \chi + \alpha_1 - 1\right]}{-\delta_1\,h_1^2 + \chi}. \tag{39}$$

The substitution of r_1 into equation (38) provides a fourth-order polynomial in δ_1, which is directly related to the frequency tuning ratio δ:

$$\tilde{a}\,\delta_1^4 + \tilde{b}\,\delta_1^3 + \tilde{c}\,\delta_1^2 + \tilde{d}\,\delta_1 + \tilde{e} = 0. \tag{40}$$

The coefficients of the polynomial depend only on α_1, related to the coupling factor α, and h_1, related to the amplitude h_0 of the receptance function:

$$\begin{aligned} \tilde{a} &= \left[h_1^4\left(1 - h_1^2\right)\right], \\ \tilde{b} &= \left[4h_1^2\left(1 - h_1^2\right)\left(\chi + \frac{1}{2}\alpha_1\right)\right], \\ \tilde{c} &= \left[\left((-4\,\chi - 2)\alpha_1 - 5\,\chi^2 + 2\right)h_1^2\right. \\ &\quad \left. + 4\left(\chi + \frac{1}{2}\,\alpha_1\right)^2 - h_1^4\right], \\ \tilde{d} &= \left[2\,\chi^3 + 2\,\chi^2\alpha_1 + \left(2\,h_1^2 + 4\,\alpha_1 - 4\right)\chi\right. \\ &\quad \left. + 2\,\alpha_1^2 - 2\,\alpha_1\right], \\ \tilde{e} &= \left[(\alpha_1 - 1)^2 - \chi^2\right]. \end{aligned} \tag{41}$$

The parameter α_1 is an input to the problem whereas h_1 should be minimized so as to minimize the resonance peak amplitude h_0.

To ensure the existence of a multiple real root of equation (40), the value of h_1 should be selected so that the discriminant of this polynomial Δ_4 is zero. For a nth-order polynomial $f(x)$, a linear relation exists between the discriminant and the resultant $R\left(f, \frac{\partial f}{\partial x}\right)$ [22]. This relation can be written for the quartic function f_2 as:

$$\Delta_4 = \frac{1}{\tilde{a}}\,R\left(f_2, \frac{\partial f_2}{\partial \delta_1}\right). \tag{42}$$

Hence, the resultant R can be set to zero instead of Δ_4. Since the expression of R is very complex and cannot be solved by hand, the symbolic algebraic software Maple is used to simplify the resultant as:

$$\begin{aligned} &\frac{1}{64}\left[54\,\alpha_1^3 - 54\,\alpha_1^2 + \left(144\,h_1^2 - 144\right)\alpha_1\right. \\ &\quad \left. - 128\,h_1^2 + 128\right]\sqrt{h_1^2 + \alpha_1^2 - 2\,\alpha_1} \\ &\quad + \frac{27}{32}\,\alpha_1^4 - \frac{27}{16}\,\alpha_1^3 + \frac{1}{64}\left(171\,h_1^2 - 117\right)\alpha_1^2 \\ &\quad + \frac{272}{64}\left(1 - h_1^2\right)\alpha_1 + h_1^4 - 1 = 0. \end{aligned} \tag{43}$$

The common factor $1024\alpha_1^4\left(h_1^2 - 1\right)^3 h_1^{10}\left[\left(h_1^2 + \chi\right)\alpha_1 - h_1^2 + \chi^2\right]^2$ was eliminated from the resultant

during the simplifications. Four different roots are found for equation (43):

$$h_1 = \pm\frac{1}{8} \times \sqrt{-9\,\alpha_1^2 - 16\,\alpha_1 + 64 \pm 2\,\sqrt{54\,\alpha_1^4 - 144\,\alpha_1^3 + 64\,\alpha_1^2}} \tag{44}$$

Considering that h_1 should be positive and should be minimized, the following root is the solution:

$$h_{1_{opt}} = \frac{1}{8} \times \sqrt{\begin{array}{l}-9\,\alpha_1^2 - 16\,\alpha_1 + 64 \\ \quad -2\,\sqrt{54\,\alpha_1^4 - 144\,\alpha_1^3 + 64\,\alpha_1^2}\end{array}}. \tag{45}$$

This value of h_1 should be inserted into equation (41) to obtain the coefficients in terms of α_1, and equation (40) can be solved analytically for δ_1. Eventually:

$$\delta_{1\mathrm{opt}} = \frac{4S\,\tilde{a} - \tilde{b}}{4\tilde{a}}. \tag{46}$$

where

$$S = \frac{1}{2}\sqrt{\frac{1}{3\tilde{a}}\left(Q + \frac{\Delta_0}{Q}\right) - \frac{2}{3}p},$$

$$p = \frac{8\tilde{a}\tilde{c} - 3\tilde{b}^2}{8\tilde{a}^2},$$

$$Q = \sqrt[3]{\frac{\Delta_1 + \sqrt{\Delta_1^2 - 4\Delta_0^3}}{2}} \tag{47}$$

while the parameters Δ_0 and Δ_1 are:

$$\Delta_0 = \tilde{c}^2 - 3\tilde{b}\tilde{d} + 12\tilde{a}\tilde{e},$$

$$\Delta_1 = 2\tilde{c}^3 - 9\tilde{b}\tilde{c}\tilde{d} + 27\tilde{b}^2\tilde{e} + 27\tilde{a}\tilde{d}^2 - 72\tilde{a}. \tag{48}$$

In summary, the solution to the tuning of the resonant shunt circuit can be written in terms of the original parameters δ, r and α by considering equations (49)–(52). From the knowledge of the coupling factor α, h_0 and χ are computed:

$$h_0 = \frac{8}{\alpha\,\sqrt{2\,\sqrt{54\,\alpha^4 - 144\,\alpha^2 + 64} + 9\,\alpha^2 + 16}}, \tag{49}$$

$$\chi = \frac{1}{8} \times \sqrt{64 - 2\,\alpha^2\sqrt{54\,\alpha^4 - 144\,\alpha^2 + 64} + 55\,\alpha^4 - 144\,\alpha^2} \tag{50}$$

To obtain real values for h_0 and χ, the allowable range of α is $\alpha \leqslant \frac{2}{53}\sqrt{954 - 212\sqrt{7}} \cong 0.748\,15$. This limit on the maximum value of α should not pose any practical difficulty since electromechanical coupling factors should usually be lower than this limit. The coefficients of the quartic

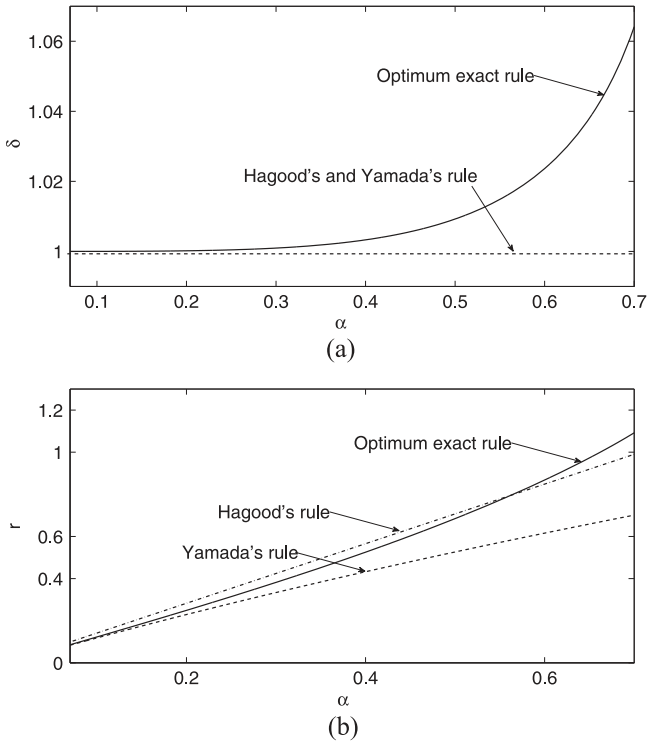

Figure 4. Variation of (a) the tuning frequency ratio δ, and (b) the dimensionless damping of the shunt r predicted by the different tuning rules against the electromechanical coupling parameter α.

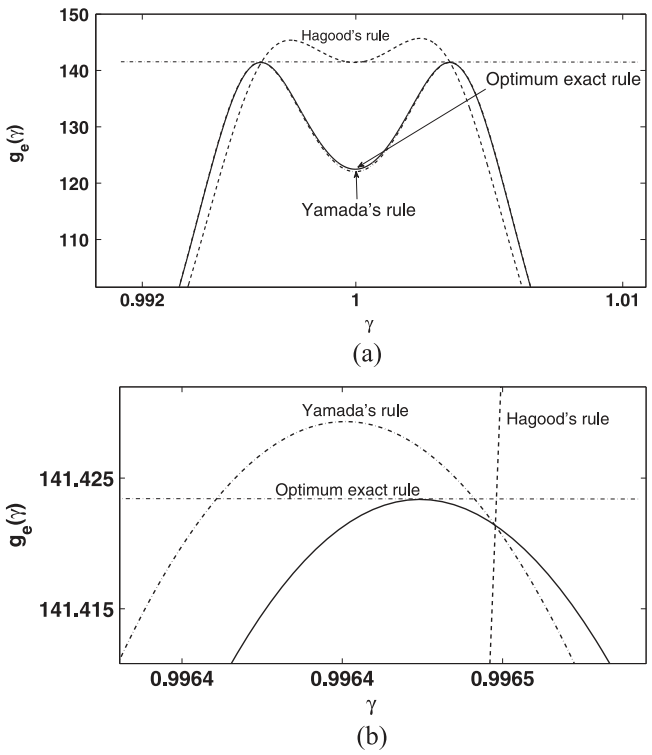

Figure 5. (a) Performance of the three tuning rules for $\alpha = 0.01$, (b) close-up of the resonant peak.

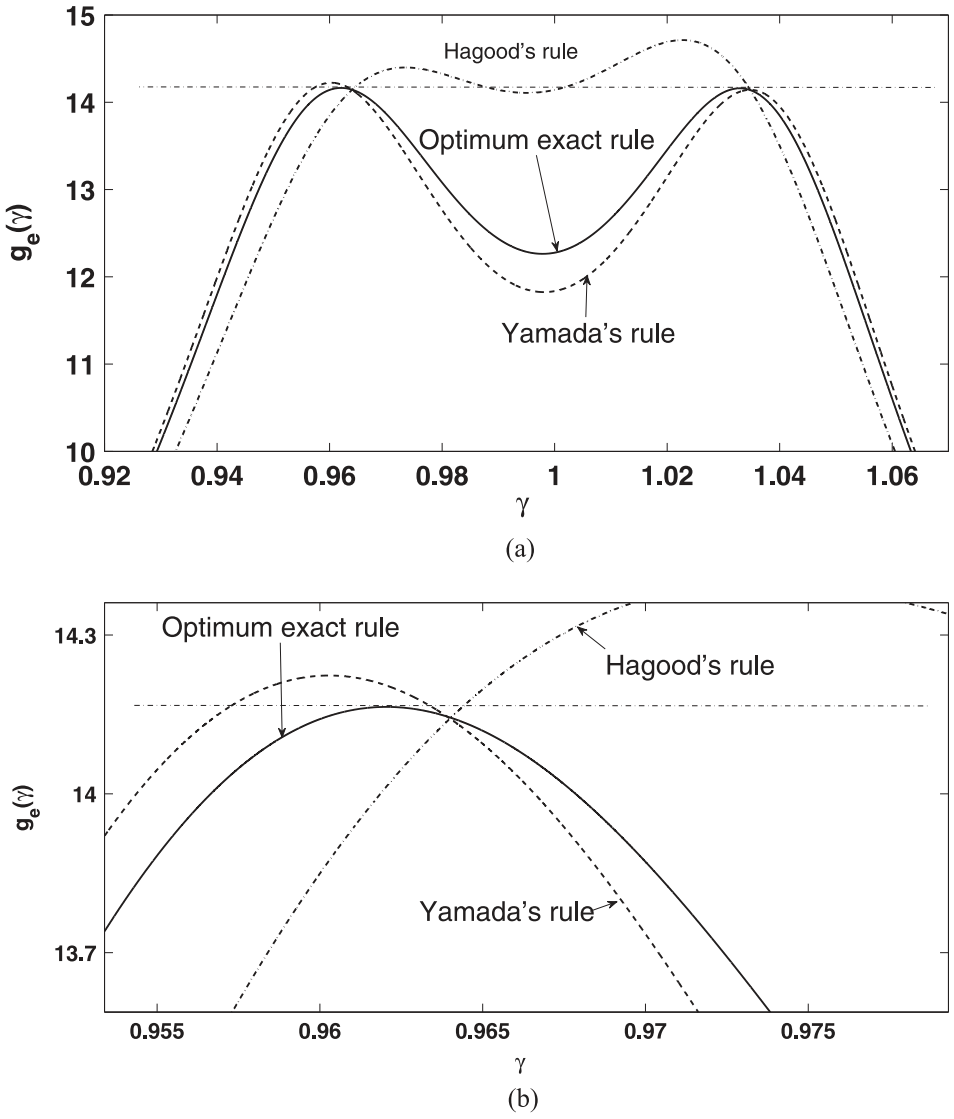

Figure 6. (a) Performance of the three tuning rules for $\alpha = 0.01$, (b) close-up of the resonant peak.

polynomials (40) are then calculated:

$$\tilde{a} = \frac{\left(h_0^2 - 1\right)^2}{h_0^6},$$

$$\tilde{b} = -2\,\frac{\left(2\,\chi + \alpha^2\right)\left(h_0^2 - 1\right)}{h_0^4},$$

$$\tilde{c} = 5\,\frac{\alpha^4}{h_0^2} + \left(\frac{4\chi}{h_0^2} - \frac{8}{h_0^2}\right)\alpha^2 + \frac{6}{h_0^2} - \frac{6}{h_0^4},$$

$$\tilde{d} = 2\,\chi^3 + \left(4\,\alpha^2 - 2 - \frac{2}{h_0^2}\right)\chi - 2\,\frac{\alpha^2}{h_0^2} + 2\,\alpha^6 - 2\,\alpha^4,$$

$$\tilde{e} = \frac{1}{h_0^2}. \tag{51}$$

From these coefficients, variables Δ_0, Δ_1, p, Q and S in equations (47) and (48) are determined. The optimal parameters can then be obtained:

$$\delta_{\text{opt}} = 2\,\sqrt{\frac{\tilde{a}}{4\,S\tilde{a} - \tilde{b}}},$$

$$r_{\text{opt}} = \sqrt{\frac{2\left[1 + \left(\delta_{\text{opt}}^2 + 1\right)\left(\alpha^2 + \chi - 1\right)h_0^2\right]}{\left[1 + \left(\chi\,\delta_{\text{opt}}^2 - 1\right)h_0^2\right]\delta_{\text{opt}}^2}}. \tag{52}$$

The resistance R and inductance L of the shunt circuit are calculated directly from r_{opt} and δ_{opt} using equations (13):

$$L = \frac{1}{\delta_{\text{opt}}^2}\,\frac{m_1}{(1+\kappa)\epsilon_3^T}\left(\frac{s_{33}\,l_0}{s_0}\right)^2 \tag{53}$$

$$R = \frac{r_{\text{opt}}}{\epsilon_3^T}\,\sqrt{\frac{m_1}{1+\kappa}}\,\sqrt{s_{33}\left(\frac{l_0}{s_0}\right)^3}. \tag{54}$$

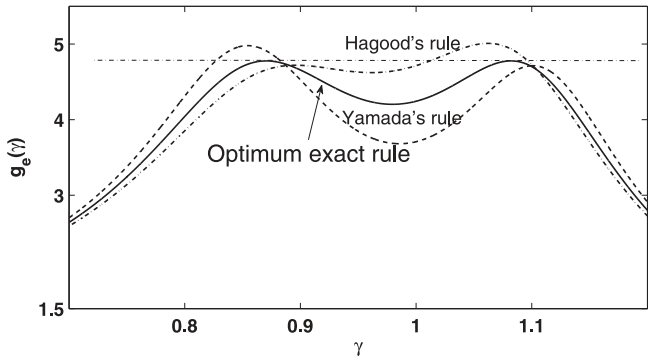

Figure 7. Performance of the three tuning rules for $\alpha = 0.3$.

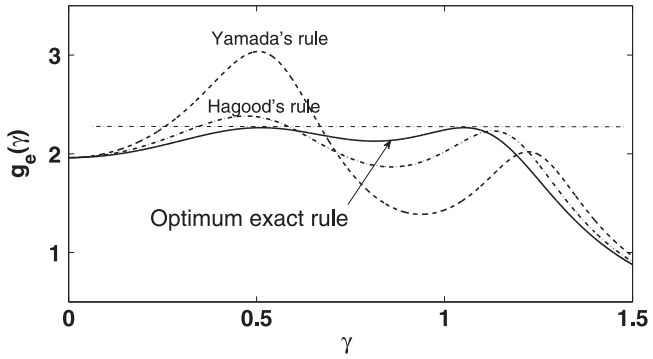

Figure 8. Performance of the three tuning rules for $\alpha = 0.7$.

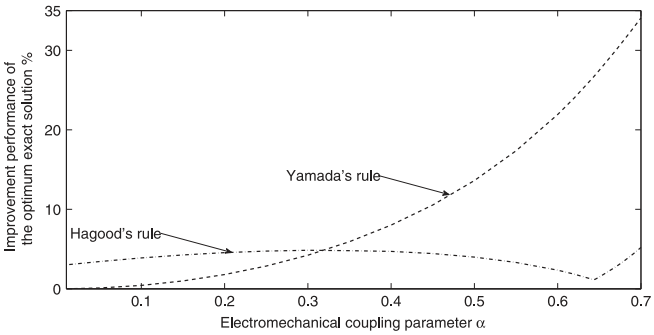

Figure 9. Percentage of peak amplitude reduction provided by the exact closed-form solution against the dimensionless coupling parameter α.

4.2. Numerical results

The transfer function of the primary oscillator (17) is computed for the optimal values proposed by the three tuning rules investigated in this paper:

$$\delta_{\mathrm{opt,H}} = \delta_{\mathrm{opt,Y}} = 1,$$

$$\delta_{\mathrm{opt,exact}} = 2\sqrt{\frac{\tilde{a}}{4\,S\tilde{a} - \tilde{b}}}, \tag{55}$$

$$r_{\mathrm{opt,H}} = \sqrt{2}\,\alpha,$$

$$r_{\mathrm{opt,Y}} = \sqrt{\frac{r_P^2 + r_Q^2}{2}} = \frac{\sqrt{3}\,\alpha}{\sqrt{2 - \alpha^2}}, \tag{56}$$

$$r_{\mathrm{opt,exact}} = \sqrt{\frac{2\left[1 + \left(\delta^2 + 1\right)\left(\alpha^2 + \chi - 1\right)h_0^2\right]}{\left[1 + \left(\chi\,\delta^2 - 1\right)h_0^2\right]\delta^2}}. \tag{57}$$

These values are plotted in figure 4 as a function of the dimensionless coupling parameter α within its allowable domain. Because a rapid computation of the optimal parameters could be useful in some applications (e.g., for potential digital implementation of the shunt circuit), very precise simplified formulas are also proposed in the appendix. figures 5–8, which depict the transfer functions for four different values of α, fully validate the analytic developments carried out in the previous section. Indeed, the transfer function for the exact rule possesses two resonance peaks with identical amplitude. The corresponding amplitude is also consistently lower than the maximum peak amplitude given by the other tuning rules.

For a very low value of the coupling parameter, $\alpha = 0.01$ in figure 5, there is almost no visible difference between Yamada and exact rules. The damping value proposed by Hagood's formula is associated with a noticeable performance decrease. For $\alpha = 0.1$ and $\alpha = 0.3$ in figures 6 and 7, respectively, both Hagood and Yamada rules lead to lower performance compared to the exact rule. Finally, for $\alpha = 0.7$ in figure 8, a complete detuning is observed for Yamada's rule. For a more quantitative comparison, figure 9 displays the percentage of peak amplitude reduction provided by the exact rule as a function of α. It confirms the superiority of this tuning methodology over the existing methods. For realistic values of α, an improvement of a couple of percents can be expected.

Table A2. The coefficients n_i in equation (A.2).

$\hat{r}$	n_3	n_2	n_1	n_0
$\alpha \leqslant 0.2$	0.5256	−0.000 92	1.2247	0
$\alpha > 0.2$	1.178 61	−0.5223	1.353 53	−0.00901

Table A1. The coefficients a_i in equation (A.1).

$\hat{\delta}$	a_5	a_4	a_3	a_2	a_1	a_0
$\alpha \leqslant 0.2$	0.092 25	0.0808	0.002 94	0	0	0
$\alpha > 0.2$	4.263 14	−6.4942	3.9275	−1.0805	0.1335	−0.005 771

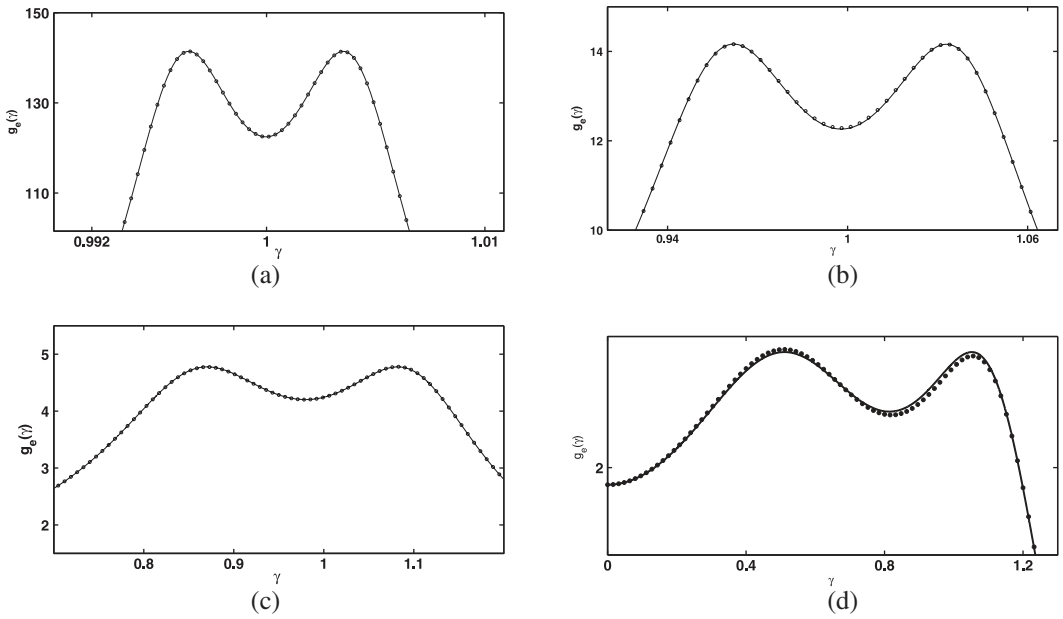

Figure A1. Receptance transfer function for the exact (solid line) and fitted (circles) values of δ_{opt} and r_{opt} for different dimensionless coupling parameters α. (a) $\alpha = 0.1$ (b) $\alpha = 0.1$ (c) $\alpha = 0.3$ (d) $\alpha = 0.7$

Table A3. Exact and fitted values of δ_{opt}, r_{opt} and h_0.

α	δ	$\hat{\delta}$	r	$\hat{r}$	h_0	$\hat{h}_0$
0.001	1.000 000 0	1.000 000 0	0.0012	0.0012	1414.2	1414.2
0.005	1.000 000 0	1.000 000 0	0.0061	0.0061	282.8433	282.8434
0.01	1.000 000 0	1.000 000 0	0.0122	0.0122	141.4233	141.4234
0.02	1.000 000 0	1.000 000 0	0.0245	0.0245	70.7146	70.7148
0.05	1.000 000 1	1.000 000 1	0.0613	0.0613	28.2942	28.2945
0.1	1.000 010 7	1.000 011 9	0.1230	0.1230	14.1621	14.1624
0.2	1.000 176 7	1.000 182 4	0.2492	0.2491	7.1118	7.1123
0.3	1.000 951 1	1.000 832 9	0.3819	0.3819	4.7772	4.7753
0.4	1.003 300 6	1.003 512 0	0.5254	0.5243	3.6242	3.6283
0.5	1.009 248 5	1.009 127 1	0.6848	0.6845	2.9482	2.9481
0.6	1.023 655 8	1.023 542 4	0.8680	0.8697	2.5200	2.5174
0.65	1.038 020 0	1.038 476 2	0.9728	0.9738	2.3705	2.3697

5. Conclusion

In this paper, an exact closed-form solution to the H_∞ optimization of piezoelectric material shunted with inductive-resistive passive electrical circuits is proposed. This solution imposes exactly two equal peaks in the receptance function that are associated with the smallest possible vibration amplitude of the host structure. The performance of this method is therefore superior to all existing tuning rules for resonant circuit shunting, even if the improvement may be marginal for small electromechanical coupling parameters. Simplified, though very accurate, formulas for the optimum tuning ratio and the dimensionless damping are also provided in the Appendix.

Acknowledgements

All authors, P Soltani, G Tondreau, A Deraemaeker and G Kerschen, would like to acknowledge the financial support of the Belgian National Science Foundation FRS-FNRS (PDR T.0028.13). The author G Kerschen would like to acknowledge the financial support of the European Union (ERC Starting Grant NoVib 307265).

Appendix. Simplification of the exact formulas

The curves $\delta_{\text{opt}} = \delta_{\text{opt}}(\alpha)$ and $r_{\text{opt}} = r_{\text{opt}}(\alpha)$ in figure 4 are fitted using fifth and third-order polynomials:

$$\hat{\delta}_{\text{opt}} = 1 + \Big(a_5\,\alpha^5 + a_4\,\alpha^4 + a_3\,\alpha^3 + a_2\,\alpha^2 + a_1\,\alpha + a_0\Big), \tag{A.1}$$

$$\hat{r}_{\text{opt}} = n_3\,\alpha^3 + n_2\,\alpha^2 + n_1\,\alpha + n_0\,. \tag{A.2}$$

The coefficients a_i ($i = 0, 1, 2,..., 5$) and n_j ($j = 0, 1, 2, 3$) are listed in tables A1 and A2, respectively.

Table A3 compares the exact and fitted values of the design parameters δ and r together with the corresponding maximum amplitude of the receptance function h_0. The maximum relative error on δ and r is 0.04% and 0.2%, respectively. Figure A1 depicts the comparison between the exact and fitted transfer functions for different dimensionless coupling parameters α. Overall, these results demonstrate the very high accuracy of the proposed simplifications (A.1)–(A.2).

References

[1] Sun J, Jolly M R and Norris M 1995 Passive, adaptive, and active tuned vibration absorbers-a survey *J. Mech. Des.* **117** 234–42

[2] den Hartog J P 1934 *Mechanical Vibrations* (New York: McGraw-Hill)

[3] Brock J 1946 A note on the damped vibration absorber *J. Appl. Mech.* **13** A284

[4] Nishihara O and Asami T 2002 Closed-form solutions to the exact optimizations of dynamic vibration absorbers (minimizations of the maximum amplitude magnification factors) *J. Vib. Acoust.* **124** 576–82

[5] Asami T, Nishihara O and Baz A 2002 Analytical solutions to H_∞ and H_2 optimization of dynamic vibration absorbers attached to damped linear systems *J. Vib. Acoust.* **124** 284–95

[6] Mohameini S 2003 A survey of recent innovations in vibration damping and control using shunted piezoelectric transducers *IEEE Trans. Control Syst. Technol.* **11** 482–94

[7] Hagood N W and von Flotow A 1991 Damping of structural vibrations with piezoelectric materials and passive electrical networks *J. Sound Vib.* **146** 243–68

[8] Preumont A 2006 *Mechatronics: Dynamics of Electromechanical and Piezoelectric Systems* (Berlin: Springer)

[9] Agnes G S and Inman D J 1996 Nonlinear piezoelectric vibration absorbers *Smart Mater. Struct.* **5** 704

[10] Zhou B, Thouverez F and Lenoir D 2014 Essentially nonlinear piezoelectric shunt circuits applied to mistuned bladed disks *J. Sound Vib.* **333** 2520–42

[11] Soltani P, Tondreau G, Deraemaeker A and Kerschen G 2014 Linear and nonlinear piezoelectric shunting strategies for vibration mitigation *MATEC Web Conf.* **16** 01007

[12] Yu H and Wang K 2007 Piezoelectric networks for vibration suppression of mistuned bladed disks *J. Vib. Acoust.* **129** 559–66

[13] Mokrani B, Bastaits R, Vigui R and Preumont A 2012 Vibration damping of turbomachinery components with piezoelectric transducers: theory and experiment *International Conf. on Noise and Vibration Engineering, (Leuven, Belgium)*

[14] Bachmann F, de Oliveira R, Sigg A, Schnyder V, Delpero T, Jaehne R, Bergamini A, Michaud V and Ermanni P 2012 Passive damping of composite blades using embedded piezoelectric modules or shape memory alloy wires: a comparative study *Smart Mater. Struct.* **21** 075027

[15] Kauffman J L and Lesieutre G A 2012 Piezoelectric-based vibration reduction of turbomachinery bladed disks via resonance frequency detuning *AIAA J.* **50** 1137–44

[16] Qureshi E M, Shen X and Chen J 2014 Vibration control laws via shunted piezoelectric transducers: a review *Int. J. Aeronaut. Space Sci.* **15** 1–19

[17] Hogsberg J and Krenk S 2012 Balanced calibration of resonant shunt circuits for piezoelectric vibration control *J. Intell. Mater. Syst. Struct.* **23** 1937–48

[18] Yamada K, Matsuhisa H, Utsuno H and Sawada K 2010 Optimum tuning of series and parallel LR circuits for passive vibration suppression using piezoelectric elements *J. Sound Vib.* **329** 5036–57

[19] Frahm H 1909 Device for damping vibrations of bodies *Tech. Rep.* 989958

[20] Ormondroyd J and den Hartog J 1928 The theory of the dynamic vibration absorber *Trans. ASME* **50** 9–22

[21] Meeker T 1996 Publication and proposed revision of ANSI/IEEE standard 176-1987, ANSI/IEEE standard on piezoelectricity *IEEE Trans. Ultrason. Ferroelectr. Frequation Control* **43** 717–72

[22] Sturmfels B 2002 *Solving Systems of Polynomial Equations* vol 97 (Providence, RI: American Mathematical Society)